Copy

NASA TM X-201

TECHNICAL MEMORANDUM

X-201

INVESTIGATION OF LOW-SUBSONIC FLIGHT CHARACTERISTICS OF A MODEL OF A FLAT-BOTTOM HYPERSONIC BOOST-GLIDE CONFIGURATION HAVING A 78° DELTA WING

By John W. Paulson and Robert E. Shanks

Langley Research Center
Langley Field, Va.

CLASSIFIED DOCUMENT - TITLE UNCLASSIFIED

NATIONAL AERONAUTICS AND SPACE ADMINISTRATION

WASHINGTON

October 1959

[redacted]

NATIONAL AERONAUTICS AND SPACE ADMINISTRATION

TECHNICAL MEMORANDUM X-201

INVESTIGATION OF LOW-SUBSONIC FLIGHT CHARACTERISTICS OF A MODEL OF A FLAT-BOTTOM HYPERSONIC BOOST-GLIDE CONFIGURATION HAVING A 78° DELTA WING*

By John W. Paulson and Robert E. Shanks

SUMMARY

An investigation of the low-subsonic stability and control characteristics of a model of a flat-bottom hypersonic boost-glide configuration having 78° sweep of the leading edge has been made in the Langley full-scale tunnel. The model was flown over an angle-of-attack range from 10° to 35°. Static and dynamic force tests were made in the Langley free-flight tunnel.

The investigation showed that the longitudinal stability and control characteristics were generally satisfactory with neutral or positive static longitudinal stability. The addition of artificial pitch damping resulted in satisfactory longitudinal characteristics being obtained with large amounts of static instability. The most rearward center-of-gravity position for which sustained flights could be made either with or without pitch damper corresponded to the calculated maneuver point. The lateral stability and control characteristics were satisfactory up to about 15° angle of attack. The damping of the Dutch roll oscillation decreased with increasing angle of attack; the oscillation was about neutrally stable at 20° angle of attack and unstable at angles of attack of about 25° and above. Artificial damping in roll greatly improved the lateral characteristics and resulted in flights being made up to 35° angle of attack.

INTRODUCTION

An investigation is being conducted by the National Aeronautics and Space Administration to provide information on the stability and control characteristics of some proposed hypersonic boost-glide configurations over the speed range from hypersonic to low-subsonic speeds. The present investigation was made to provide some information at low-subsonic speeds on the longitudinal and lateral stability and control characteristics of a model of a flat-bottom hypersonic boost-glide configuration having a leading-edge sweep of 78°.

*Title, Unclassified.

[redacted]

The investigation included flight tests in the Langley full-scale tunnel to determine the low-subsonic flight characteristics of the model over an angle-of-attack range from 10° to 35° and force tests in the Langley free-flight tunnel to determine the static and dynamic stability and control characteristics over an angle-of-attack range from -4° to 40°.

Included in the investigation were tests to determine the effect of center-of-gravity location on the longitudinal stability and control characteristics. These tests were made at an angle of attack of 16° with and without artificial damping in pitch added. Also studied in the flight tests was the effect of artificial roll damping on the lateral stability and control characteristics.

SYMBOLS

All velocities, forces, and moments with the exception of lift and drag were determined with respect to the body-axes system originating at the reference center-of-gravity position located at 40 percent of the mean aerodynamic chord. (See fig. 1.) The term "in phase" derivative used in this report refers to any one of the stability derivatives which are based on the forces or moments in phase with the angle of roll, yaw, or sideslip produced in the oscillatory tests. The term "out of phase" derivative refers to any one of the stability derivatives which are based on the forces or moments 90° out of phase with the angle of roll, yaw, or sideslip.

X,Y,Z	body reference axes unless otherwise noted
S	wing area (no cones), sq ft
b	wing span (no cones), ft
$\bar{c}$	mean aerodynamic chord, ft
t	time
V	free-stream velocity, ft/sec
q	free-stream dynamic pressure, lb/sq ft
ρ	air density, slugs/cu ft
m	mass, slugs
ω	angular velocity, $2\pi f$, radian/sec

f	frequency of the oscillation, cps
k	reduced frequency parameter, $\omega b/2V$
α	angle of attack, deg
β	angle of sideslip, deg or radians
δ	control deflection, deg
I_X	moment of inertia about longitudinal body axis, slug-ft^2
I_Y	moment of inertia about lateral body axis, slug-ft^2
I_Z	moment of inertia about normal body axis, slug-ft^2
p,q,r	rolling, pitching, and yawing velocity, respectively, radians/sec
$\dot{\beta} = \frac{d\beta}{dt}$	
$\dot{r} = \frac{dr}{dt}$	
$\dot{p} = \frac{dp}{dt}$	
F_L	lift, lb
F_D	drag, lb
F_Y	side force, lb
M_Y	pitching moment, ft-lb
M_X	rolling moment, ft-lb
M_Z	yawing moment, ft-lb
C_L	lift coefficient, F_L/qS

[redacted]

C_D drag coefficient, F_D/qS

C_Y side-force coefficient, F_Y/qS

C_m pitching-moment coefficient, $M_Y/qS\bar{c}$

C_l rolling-moment coefficient, M_X/qSb

C_n yawing-moment coefficient, M_Z/qSb

$C_{l_\beta} = \frac{\partial C_l}{\partial \beta}$ per deg or per radian

$C_{n_\beta} = \frac{\partial C_n}{\partial \beta}$ per deg or per radian

$C_{Y_\beta} = \frac{\partial C_Y}{\partial \beta}$ per deg or per radian

$C_{l_r} = \frac{\partial C_l}{\partial\left(\frac{rb}{2V}\right)}$

$C_{n_r} = \frac{\partial C_n}{\partial\left(\frac{rb}{2V}\right)}$

$C_{Y_r} = \frac{\partial C_Y}{\partial\left(\frac{rb}{2V}\right)}$

$C_{l_p} = \frac{\partial C_l}{\partial\left(\frac{pb}{2V}\right)}$

$C_{m_q} = \frac{\partial C_m}{\partial\left(\frac{qb}{2V}\right)}$

[redacted]

$$C_{n_p} = \frac{\partial C_n}{\partial\left(\frac{pb}{2V}\right)}$$

$$C_{Y_p} = \frac{\partial C_Y}{\partial\left(\frac{pb}{2V}\right)}$$

$$C_{l_{\dot{\beta}}} = \frac{\partial C_l}{\partial\left(\frac{\dot{\beta}b}{2V}\right)}$$

$$C_{n_{\dot{\beta}}} = \frac{\partial C_n}{\partial\left(\frac{\dot{\beta}b}{2V}\right)}$$

$$C_{Y_{\dot{\beta}}} = \frac{\partial C_Y}{\partial\left(\frac{\dot{\beta}b}{2V}\right)}$$

$$C_{l_{\dot{r}}} = \frac{\partial C_l}{\partial\left(\frac{\dot{r}b^2}{4V^2}\right)}$$

$$C_{n_{\dot{r}}} = \frac{\partial C_n}{\partial\left(\frac{\dot{r}b^2}{4V^2}\right)}$$

$$C_{Y_{\dot{r}}} = \frac{\partial C_Y}{\partial\left(\frac{\dot{r}b^2}{4V^2}\right)}$$

$$C_{l_{\dot{p}}} = \frac{\partial C_l}{\partial\left(\frac{\dot{p}b^2}{4V^2}\right)}$$

$$C_{n_{\dot{p}}} = \frac{\partial C_n}{\partial\left(\frac{\dot{p}b^2}{4V^2}\right)}$$

$$C_{Y_{\dot{p}}} = \frac{\partial C_Y}{\partial\left(\frac{\dot{p}b^2}{4V^2}\right)}$$

Subscripts:

e	elevator
a	aileron
r	rudder

APPARATUS AND TESTING TECHNIQUE

Model

The model used in the investigation was constructed at the Langley Research Center and was assumed to be a 1/10-scale model of a hypersonic boost-glide configuration. A three-view drawing of the model is shown in figure 2, and a photograph of the model flying in the full-scale tunnel is shown in figure 3. Table I gives the dimensional and mass characteristics of the model. Elevons consisting of plain flaps were used for elevator and aileron controls and all-movable upper and lower vertical tails were used for rudder control. The wing-tip-mounted cones which were intended for control at hypersonic speeds were fixed during the low-subsonic tests.

For the flight tests, thrust was provided by compressed air supplied through flexible hoses to two nozzles at the rear of the fuselage. The amount of thrust could be varied and the maximum output per nozzle was about 10 to 12 pounds. The controls were operated remotely by pilots by means of flicker (full on or off) pneumatic servomechanisms which were actuated by electric solenoids. Artificial stabilization in roll and pitch was provided by simple rate dampers. An air-driven rate gyroscope was the sensing element and the signal was fed into a servoactuator which deflected the elevons in proportion to rolling or pitching velocity. The manual control was superimposed on the control deflection resulting from the rate signal.

Test Equipment and Setup

The static and dynamic force tests were conducted in the Langley free-flight tunnel. The model was sting mounted, and the forces and moments were measured about the body axes by using internal strain-gage balances. A detailed description of the dynamic-force-test equipment and the method of obtaining the data are presented in reference 1.

The flight investigation was conducted in the Langley full-scale tunnel with the test setup illustrated in figure 4. In this setup there is an overhead safety cable to prevent the model from crashing. Combined with this cable is another cable composed of plastic hoses and wires which provide the compressed air for model thrust and power for the model control actuators. These cables are attached to the model at about the center-of-gravity location. The pitch pilot, located at the side of the test section, controls the pitching motions of the model. The thrust controller, who is also located at the side of the test section, varies the thrust of the model by remotely controlling the airflow to the model by means of a valve located at the top of the entrance cone. The thrust controller and pitch pilot coordinate their efforts in order to maintain steady flight. Another operator adjusts the safety cable so as to keep it slack during flight and takes up the slack to prevent the model from crashing if it goes out of control. A second pilot who controls the rolling and yawing motions of the model is located near the bottom of the exit cone. Motion-picture records of the flights are obtained with cameras located at the side of the test section and at the top and bottom of the exit cone.

The flight-test technique employed with this setup may be explained by describing a typical flight: A flight is started with the model being towed by the safety cable. When the tunnel speed reaches the flying speed of the model, the model thrust is increased until the flight cable becomes slack. Adjustments to the elevator and thrust are then made, if necessary, to trim the model for the particular airspeed. The flight is then continued to higher or lower airspeeds by changing the trim setting of the elevator and making the necessary adjustments to tunnel speed and model thrust to maintain steady flight.

STABILITY AND CONTROL PARAMETERS OF FLIGHT-TEST MODEL

The force tests were made to determine the static longitudinal and lateral stability and control characteristics and the oscillatory lateral stability derivatives of the model. The static tests were run at a dynamic pressure of 3.2 pounds per square foot which corresponds to an airspeed of 52 feet per second at standard sea-level conditions and to

a test Reynolds number of 1.66×10^6 based on the mean aerodynamic chord of 5.06 feet. The oscillatory tests were run at a dynamic pressure of 4.2 which corresponds to a Reynolds number of 1.9×10^6.

Static Longitudinal Stability and Control

The static longitudinal stability and control tests were made for an angle-of-attack range from -4° to 40° with wing-tip cones on and off for elevator deflections of 0°, -10°, and -20°. The effect of elevator deflection on the longitudinal characteristics of the model with cones on is shown in figure 5. These data show that the longitudinal stability of the model gradually decreases over the angle-of-attack range up to 24° and then increases rather sharply before becoming unstable at angles of attack above 28°. These data also show that elevator deflection produces a nearly constant increment of pitching moment over the angle-of-attack range and has an appreciable effect on the lift coefficient.

The effect of elevator deflection on the longitudinal characteristics of the model with cones off is shown in figure 6. From these data it is seen that the pitching-moment curves are more linear than those for the model with cones on. A comparison of these data with those of figure 5 shows that the cones increased the longitudinal stability from -4° to 12° angle of attack and from 24° to 28° angle of attack, but the cones did not affect the stability in the 12° to 24° angle-of-attack range. In general, the cones had only a small effect on the lift and elevator characteristics.

Static Lateral Stability and Control

The static lateral stability tests were run over a range of sideslip angle from 20° to -20° for angles of attack from 0° to 36° except for the cones-off configuration which was tested only up to 32° angle of attack. These tests were made with the complete model, with the model with cones off, with the model with vertical tail off, and with the model with cones and vertical tail off; the data are presented in figures 7 to 10 as the variation of the coefficients C_Y, C_n, and C_l with angle of sideslip for various angles of attack. These data are summarized in figure 11 as the variation with angle of attack of the side-force parameter C_{Y_β}, the directional-stability parameter C_{n_β}, and the effective dihedral parameter C_{l_β}, which were obtained by measuring the slopes of the curves between -5° and 5° angle of sideslip. Since some of the data in figures 7(a) to 7(d) are nonlinear with angle of sideslip, the derivative

data shown in figure 8 should be used only as an indication of trends in the data. The data of figure 8 show that the directional stability of all configurations tested gradually increased with angle of attack up to about 24° angle of attack and then increased very rapidly to 32° angle of attack before decreasing. The data show that the vertical tails were generally more effective than the cones in producing directional stability. The positive effective dihedral parameter was not greatly affected by configuration and increased rapidly to very high values as the angle of attack increased.

L 4 5 2 The aileron control effectiveness of the complete model is shown in figure 9. These data show that the rolling moments produced by the ailerons decreased by almost 50 percent as the angle of attack increased while the favorable yawing moment produced by the ailerons approximately doubled over the same angle-of-attack range.

Oscillatory Lateral Stability Derivatives

Rotary and linear oscillation tests were made to determine the oscillatory lateral stability derivatives of the model with cones off. The rotary tests were made for values of the reduced-frequency parameter k of 0.06, 0.11, and 0.17 and the linear tests were made for values of k of 0.08, 0.12, and 0.16.

The variations of the out-of-phase derivatives with angle of attack are shown in figure 10 for each value of the reduced-frequency parameter. These data show that the damping derivatives $C_{n_r} - C_{n_{\dot{\beta}}} \cos \alpha$ and $C_{l_p} + C_{l_{\dot{\beta}}} \sin \alpha$ became positive (unstable) above about 20° to 25° angle of attack. The data also show that frequency affected the values of the derivatives but generally did not change the trends.

The variation of the in-phase derivatives with angle of attack is shown in figure 11. These data show relatively small effects of frequency and are in fair agreement with the static data of figure 8.

In order to obtain the most reliable results in lateral stability calculations, derivatives such as C_{n_r} and $C_{n_{\dot{\beta}}}$ should be used independently in the equations rather than in the combination form $C_{n_r} - C_{n_{\dot{\beta}}} \cos \alpha$. Since in this investigation $\dot{\beta}$ derivatives as well as the combination derivatives were measured for most of the configurations tested, it is possible to break up the combination derivatives into their component parts. The values of C_{n_p}, C_{l_p}, C_{n_r}, and C_{l_r} presented in figure 12 were therefore obtained by taking the difference between the $\dot{\beta}$

[redacted]

and combination derivatives presented in figure 10. In general, the data of figure 12 show systematic variations over the angle-of-attack range which are similar to those of the combination derivatives.

FLIGHT TESTS

Flight tests were made to determine the dynamic stability and control characteristics of the model over an angle-of-attack range from 10° to 35°. The model was tested with cones on and off and with the vertical tail on and off. Flights were made at 16° angle of attack with the cones off to determine the effect of center-of-gravity position on the longitudinal characteristics of the model with and without artificial pitch damping added. Flights were also made over the angle-of-attack range to determine the effect of artificial roll damping on the lateral stability and control characteristics.

Flights were made with coordinated aileron and rudder control and also with ailerons alone. The control deflections used for most of the flight tests were $\delta_a = \pm 5^\circ$, $\delta_r = \pm 10^\circ$, and $\delta_e = \pm 5^\circ$ or $\pm 2^\circ$.

The model behavior during flight was observed by the pitch pilot located at the side of the test section and by the roll and yaw pilot located in the rear of the test section. The results obtained in the flight tests were primarily in the form of qualitative ratings of flight behavior based on pilot opinion. The motion-picture records obtained in the tests were used to verify and correlate the ratings for the different flight conditions.

FLIGHT-TEST RESULTS AND DISCUSSION

A motion-picture film supplement covering flight tests of the model has been prepared and is available on loan. A request card form and a description of the film will be found at the back of this paper on the page immediately preceding the abstract and index page.

Longitudinal Stability and Control

During the investigation made to study the longitudinal stability and control characteristics of the model, artificial damping in roll was used in order to minimize any effects lateral motions might have on the longitudinal behavior.

Summarized in figure 13 in the form of flight ratings are the results of the longitudinal investigation made at 16° angle of attack on the model with the cones off to determine the effect of center-of-gravity location. Shown in the figure are the flight ratings as a function of center-of-gravity location for the model with and without pitch damper. Also shown in figure 13 is the aerodynamic-center location as measured in static force tests (42 percent of the mean aerodynamic chord) and the estimated maneuver-point location based on the damping-in-pitch values for the model without and with pitch damper (46 to 51 percent of the mean aerodynamic chord). The increment between the aerodynamic center and the maneuver point was obtained from the expression $\frac{dC_m}{dC_L} = -\left(\frac{1}{4}\frac{\rho S\bar{c}}{m}\right)C_{m_q}$ which can be derived from equation (9) of reference 2. The values of inherent C_{m_q} shown in figure 13 were obtained by adjusting the experimental value given in reference 3 (for model 4) to the test configuration by using force-test data on the model. The variation of C_{m_q} with center-of-gravity position was obtained by using equation (2) of reference 3.

No pitch damping added.- It is seen from figure 13 that for center-of-gravity positions ahead of the aerodynamic center (42 percent of the mean aerodynamic chord) the model without added pitch damping was easy to fly and the pilot had no trouble controlling it. With neutral stability, the model was still easy to fly although it did require somewhat more attention on the part of the pilot to keep it flying smoothly. With the center of gravity at 45 percent of the mean aerodynamic chord the model reacted rather sharply to gusts and control disturbances and the pilot had to pay very close attention to the elevator control at all times to keep the model flying. This was considered to be the most rearward center-of-gravity position at which sustained flights could be made. When the center of gravity was moved rearward of the 45-percent position the model could be flown as long as it did not become badly disturbed, but the controls were not powerful enough to prevent the model from diverging in pitch once it was disturbed. It can be seen from figure 13 that the most rearward center-of-gravity position for which sustained flights could be made corresponded approximately to the maneuver point. This result is in general agreement with results that have been obtained in flight tests of airplanes in the past.

It was found in the flight tests with the elevator deflection reduced from ±5° to ±2° that sustained flights could not be achieved with the center of gravity any farther rearward than 42 percent of the mean aerodynamic chord, which indicates, to some extent at least, that the amount of instability which could be tolerated was a function of the total pitching moment used for control.

In addition to the studies made at 16° angle of attack for various locations of the center of gravity, flights were made from 10° to 30° angle of attack at a center-of-gravity position of 38 percent $\bar{c}$. The longitudinal characteristics of the model with cones on or off were generally satisfactory at angles of attack up to about 30° where the model had a pitch-up tendency. Although the pitch up was fairly mild, careful attention to control was required to prevent the model from nosing up and diverging in pitch.

Pitch damping added.- In order to determine the effect of additional pitch damping on the longitudinal behavior of the model, flight tests were made with damping in pitch increased by about -1.9 by a rate damper. The flight ratings summarized in figure 13 show that the center-of-gravity range that could be flown was greatly increased by the addition of artificial damping. Sustained flights were obtained with the center of gravity at 51 percent of the mean aerodynamic chord which was the maneuver point for this condition. The behavior of the model with this center-of-gravity position was comparable to that of the basic model with the center of gravity located at 45 percent of the mean aerodynamic chord. In other words, as in the case of the flight tests without pitch damper, the calculated maneuver point provided a good indication of the most rearward center-of-gravity position for which sustained flights could be made.

L 4 5 2

Although it would appear unlikely that an unstable condition could be tolerated in an operational airplane because of the close attention to control required of the pilot, it does seem possible on the basis of the present pitch-damper studies and the analog studies of reference 4 that a basically unstable airplane might be made acceptable through the addition of artificial damping in pitch.

Lateral Stability and Control

No roll damping added.- The lateral stability and control characteristics of the model were considered to be good at the lower angles of attack flown (10° to 15°). The model was easy to control and flew smoothly despite the fact that the Dutch roll oscillation was lightly damped. As the angle of attack was increased, the oscillation became less damped and at about 20° angle of attack the model had a constant-amplitude Dutch roll oscillation. The model could still be controlled satisfactorily in this angle-of-attack range and the oscillation could be stopped by proper use of the controls. As the angle of attack increased to about 25° the oscillation became unstable and the model went out of control despite the efforts of the pilot to control it. One factor probably contributing to this behavior is that the damping derivatives became unstable above 20° angle of attack. (See fig. 10.) Because of the large ratios of I_Z/I_X and C_{l_β}/C_{n_β} for this model the oscillation appeared to be a pure rolling motion about the body axis.

The flight tests showed that with the tip cones removed the model motions during an oscillation were slightly faster, apparently because of the reduced rolling inertia, and the model was a little more difficult to control.

Roll damping added.- The addition of rate roll damping to improve the stability of the Dutch roll oscillation greatly improved the lateral characteristics of the model so that flights were made to higher angles of attack. The Dutch roll oscillation was made very stable at 25° angle of attack with $\Delta C_{l_p} = -0.3$ added, but the oscillation again became unstable even with the added damping at about 30° angle of attack. With a further increase in ΔC_{l_p} to -0.4 the model was flown up to maximum lift ($\alpha = 35°$).

During flights with rudder fixed and ailerons alone used for control the behavior of the model was generally similar to that of the model with coordinated ailerons and rudder except that without the rudder control it was more difficult to recover the model from a disturbance. This was particularly true whenever there were any sidewise motions of the model. In this case the lag between the application of aileron control and the response of the model to the angle of bank resulted in the model being slow to return to the desired position in the tunnel. In flights made from 24° to 29° angle of attack with the vertical tails removed, the lateral stability characteristics were still generally similar to those for the case with rudder fixed and ailerons alone used for control.

CONCLUSIONS

The results of a low-subsonic investigation of the stability and control characteristics of a free-flying model of a flat-bottom hypersonic boost-glide configuration can be summarized as follows:

1. The longitudinal stability and control characteristics of the basic model were satisfactory when the model had positive or neutral static longitudinal stability, and flights could be maintained with a small amount of static instability. Adding artificial pitch damping resulted in satisfactory flights being obtained with large amounts of static instability. The most rearward center-of-gravity position for which sustained flights could be made either with or without pitch damper corresponded to the calculated maneuver point. The model had a mild pitch-up tendency near 30° angle of attack which could be controlled by the pilot.

2. The lateral stability and control characteristics were considered to be satisfactory at the lower angles of attack flown (α = 10° to 15°). The damping of the Dutch roll oscillation decreased with increasing angle of attack; the oscillation was about neutrally stable at 20° angle of attack and unstable at angles of attack of 25° and above. Artificial damping in roll greatly improved the lateral characteristics and resulted in flights being made up to 35° angle of attack.

Langley Research Center,
National Aeronautics and Space Aministration,
Langley Field, Va., April 28, 1959.

REFERENCES

1. Hewes, Donald E.: Low-Subsonic Measurements of the Static and Oscillatory Lateral Stability Derivatives of a Sweptback-Wing Airplane Configuration for Angles of Attack From -10° to 90°. NASA MEMO 5-20-59L, 1959.

2. Donlan, C. J., and Recant, I. G.: Methods of Analyzing Wind-Tunnel Data for Dynamic Flight Conditions. NACA TN 828, 1941.

3. Goodman, Alex, and Jaquet, Byron M.: Low-Speed Pitching Derivatives of Low-Aspect-Ratio Wings of Triangular and Modified Triangular Plan Forms. NACA RM L50C02, 1950.

4. Moul, Martin T., and Brown, Lawrence W.: Effect of Artificial Pitch Damping on the Longitudinal and Lateral Stability of Aircraft With Negative Static Margins. NASA MEMO 5-5-59L, 1959.

TABLE I.- GEOMETRIC AND MASS CHARACTERISTICS OF TEST MODEL

Gross weight (cones on), lb	33
I_X, slug-ft^2	0.5
I_Y, slug-ft^2	4.8
I_Z, slug-ft^2	4.9
Wing:	
Airfoil section	3.25-percent-thick wedge
Area (no cones), sq ft	11.7
Span (no cones), sq ft	2.95
Aspect ratio (no cones)	0.74
Root chord, ft	7.5
Tip chord, ft	0
Mean aerodynamic chord, ft	5.06
Sweep of leading edge, deg	78
Dihedral lower surface, deg	8.6
Dihedral upper surface, deg	0
Leading-edge diameter, ft	0.01
Fins (each):	
Airfoil section	5.6-percent-thick wedge
Span (from fuselage to tip), ft	0.41
Aspect ratio	0.55
Root chord, ft	1.48
Tip chord, ft	0
Mean aerodynamic chord, ft	0.99
Sweep of leading edge, deg	75
Leading-edge diameter, ft	0.01
Cones:	
Length, ft	1.52
Diameter, ft	0.40
Apex angle, deg	15

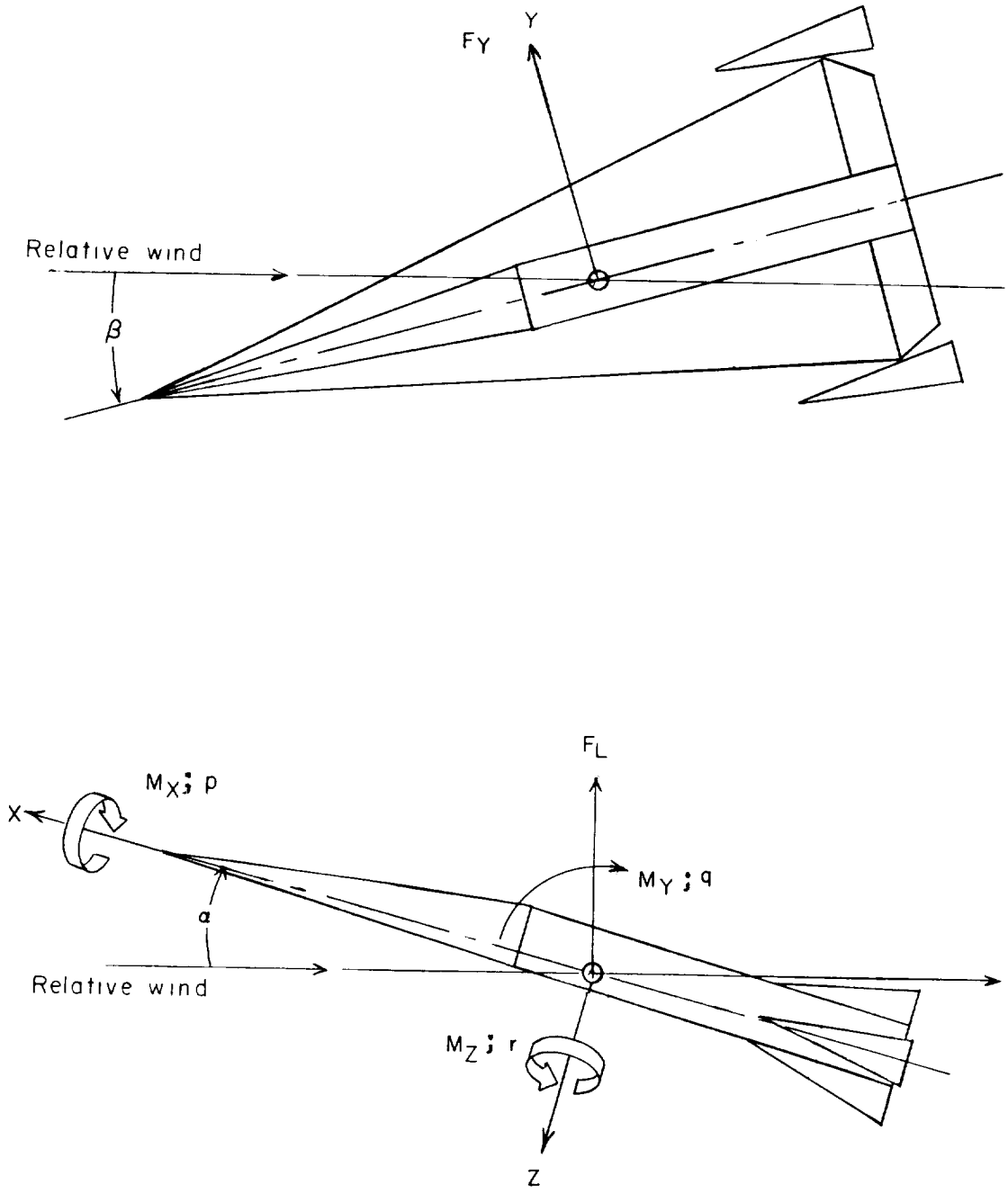

Figure 1.- Sketch of body system of axes showing positive direction of forces, moments, velocities, and angles.

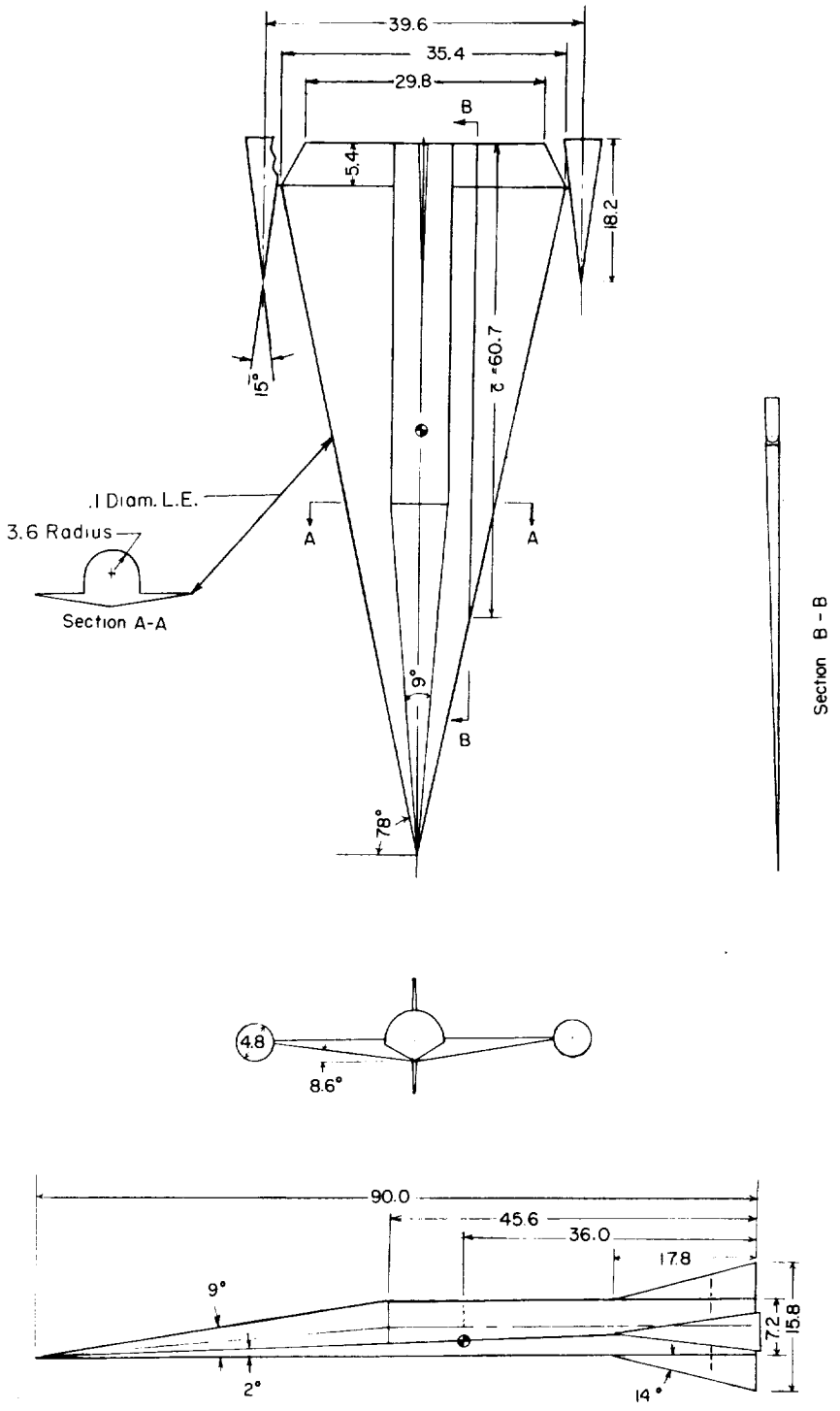

Figure 2.- Three-view drawing of model used in investigation. All dimensions are in inches.

Figure 3.- Model flying in Langley full-scale tunnel. L-57-1440

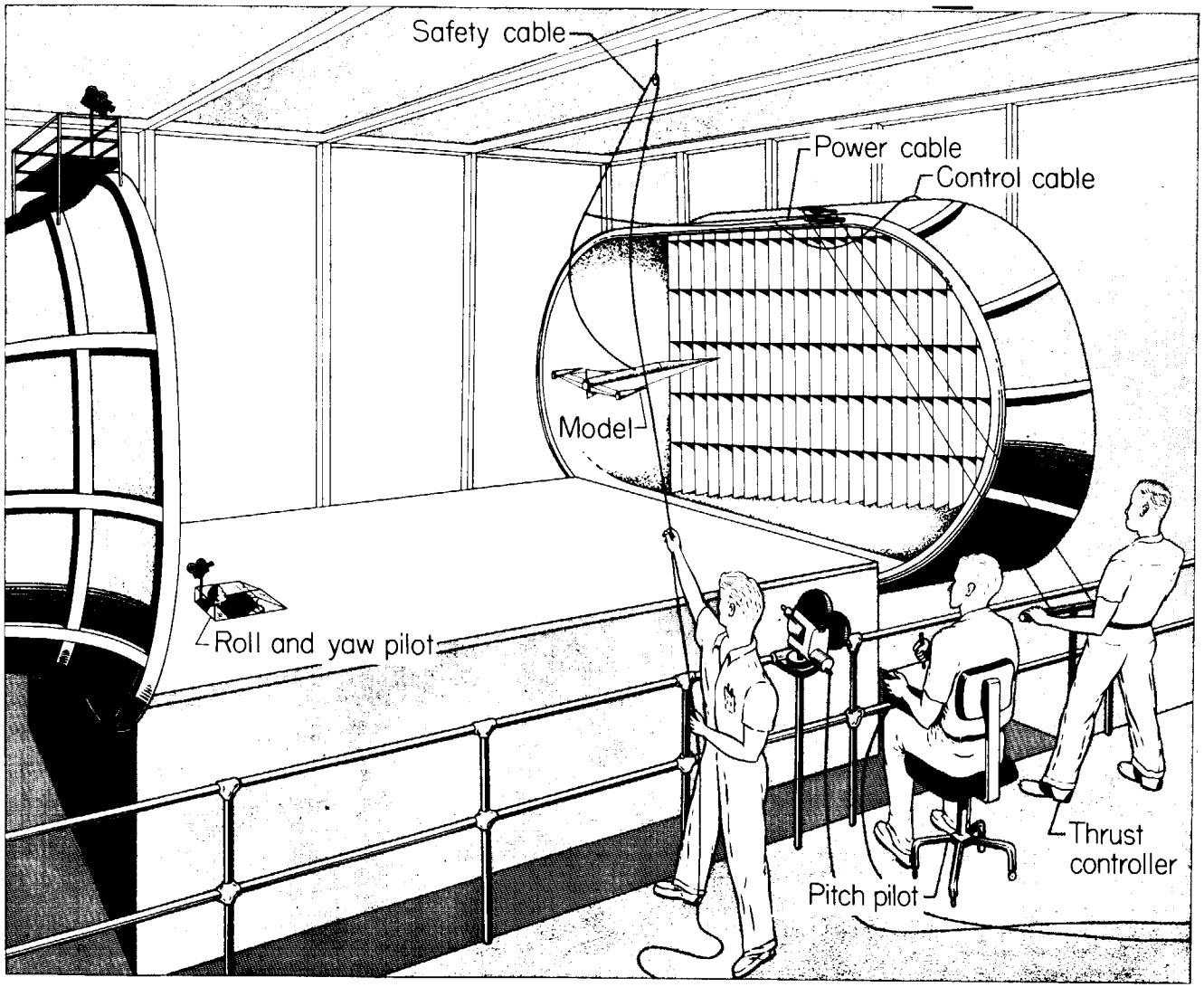

Figure 4.- Flight-test setup in Langley full-scale tunnel.

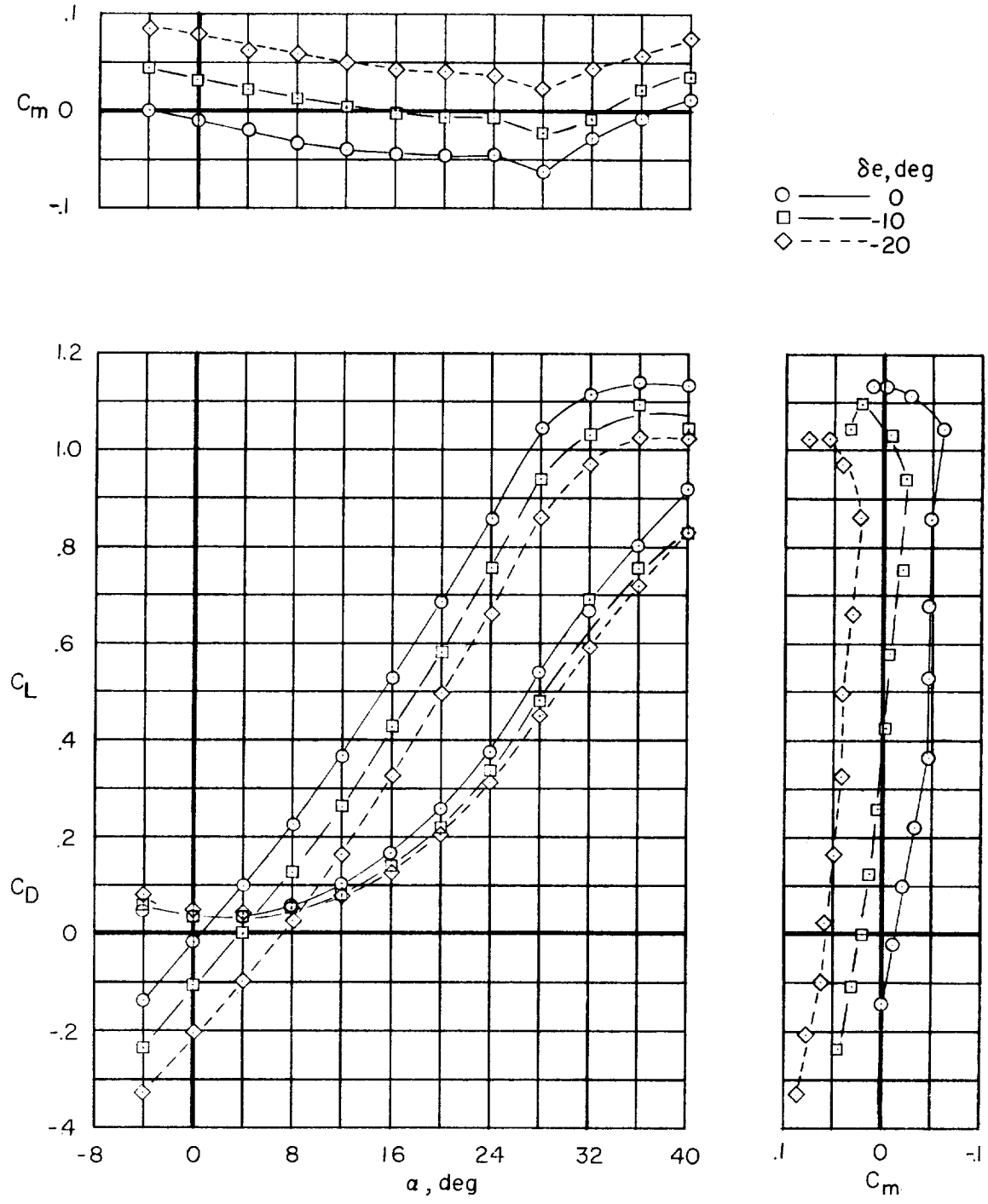

Figure 5.- Effect of elevator deflection on longitudinal characteristics of model with cones on. $\beta = 0^{\circ}$.

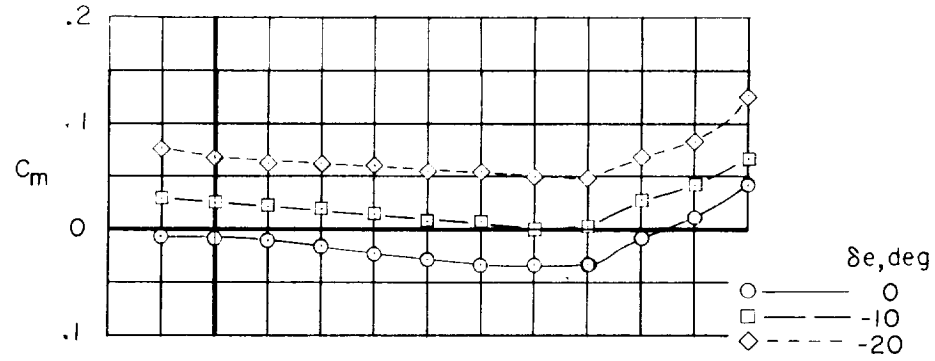

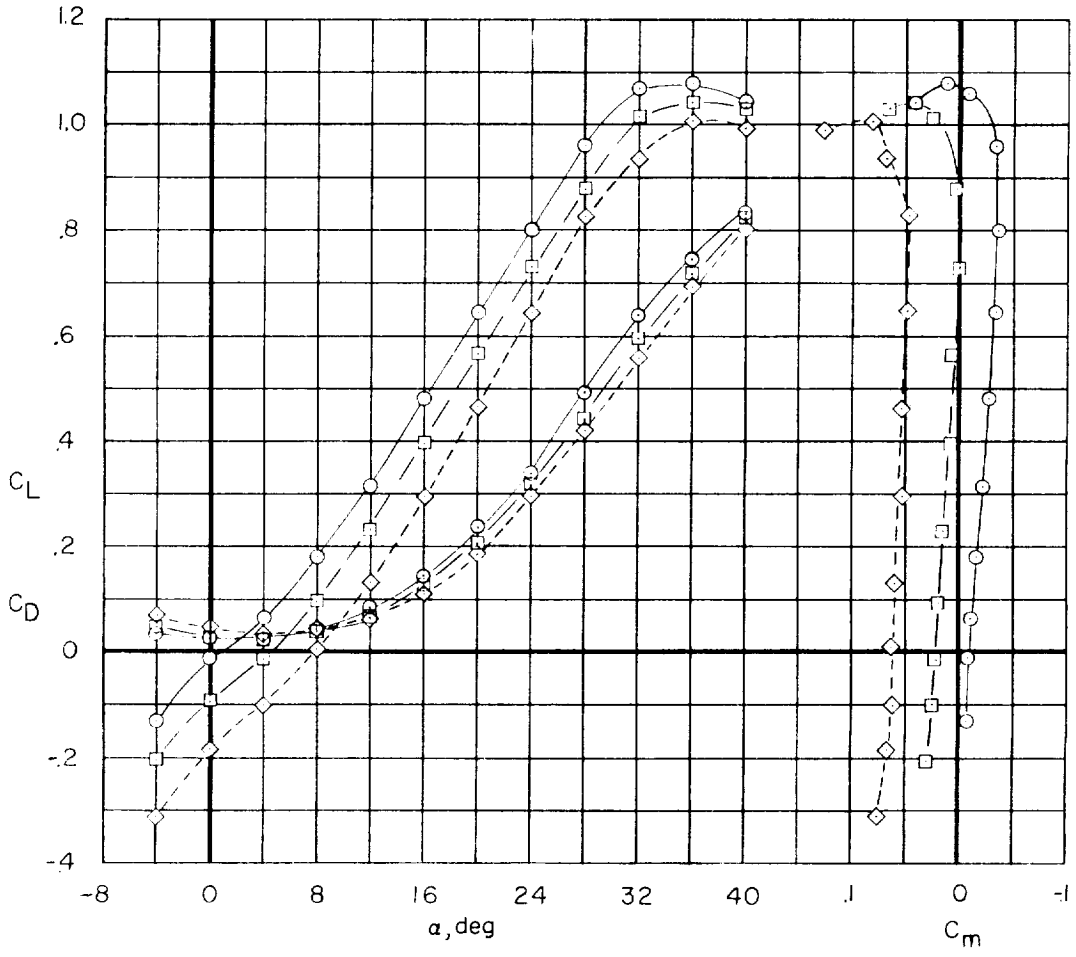

Figure 6.- Effect of elevator deflection on longitudinal characteristics of model. Cones off; $\beta = 0^{\circ}$.

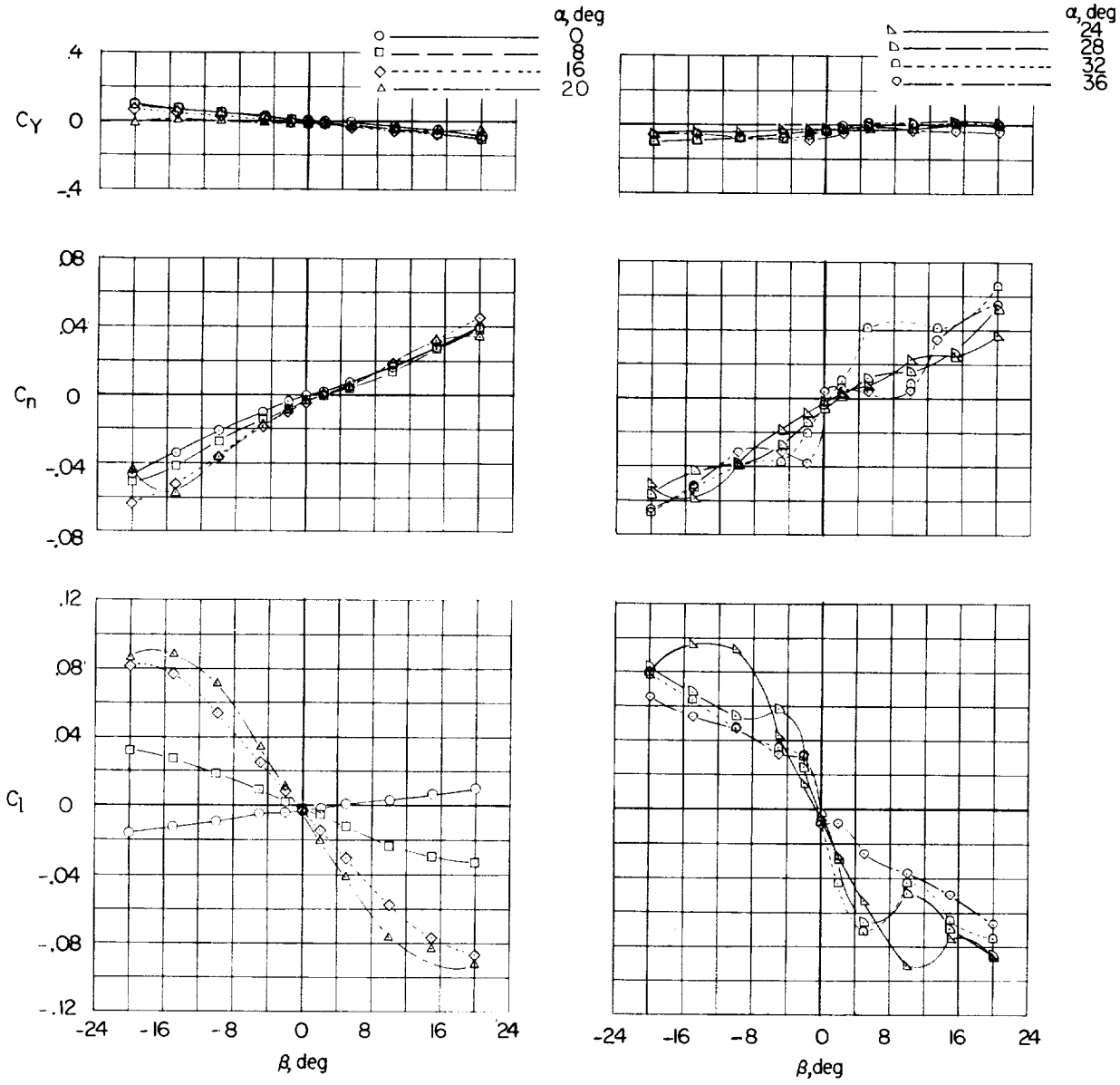

(a) Cones on.

Figure 7.- Variation of static lateral stability coefficients with angle of sideslip. $\delta_e = 0^\circ$.

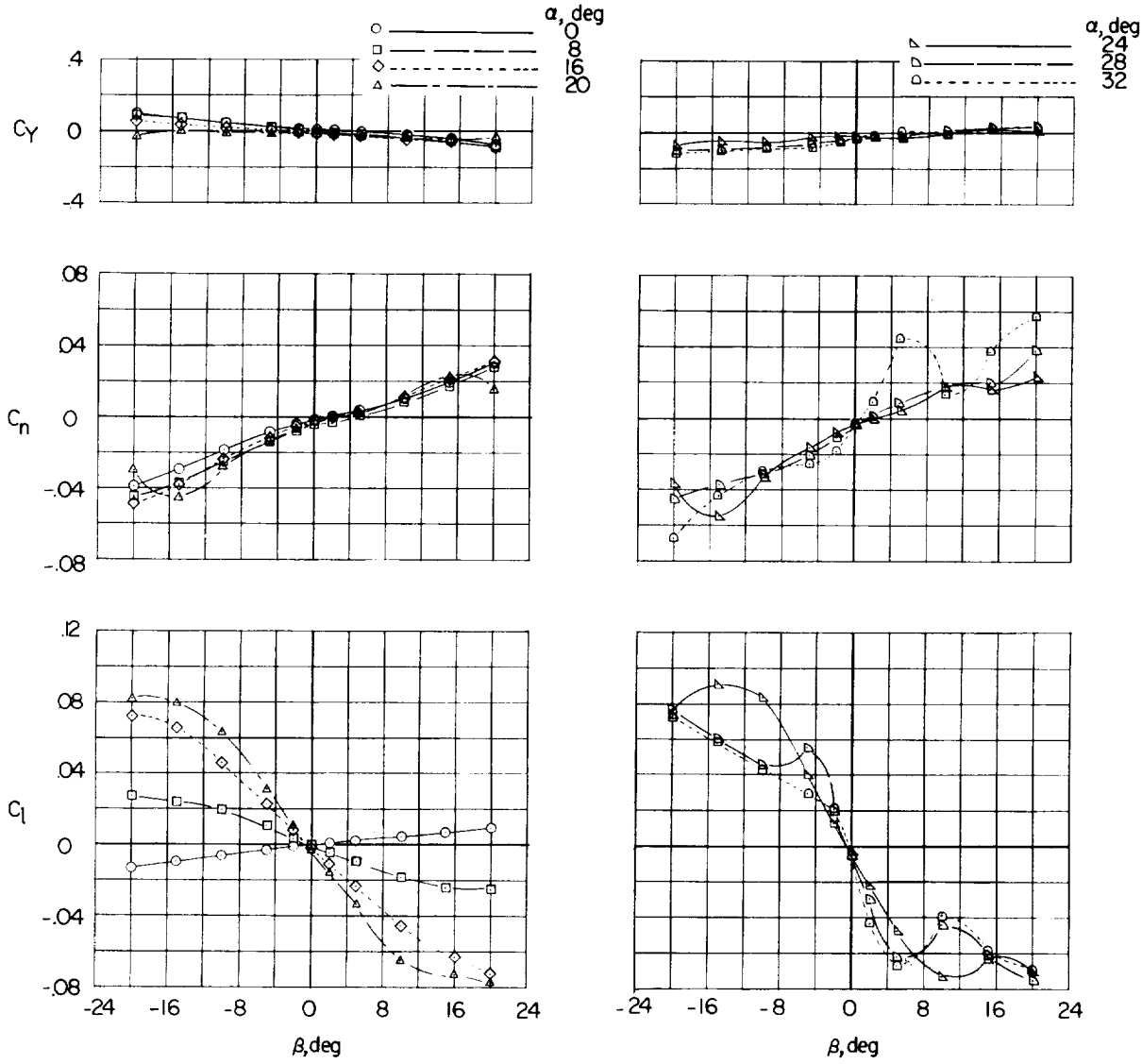

(b) Cones off.

Figure 7.- Continued.

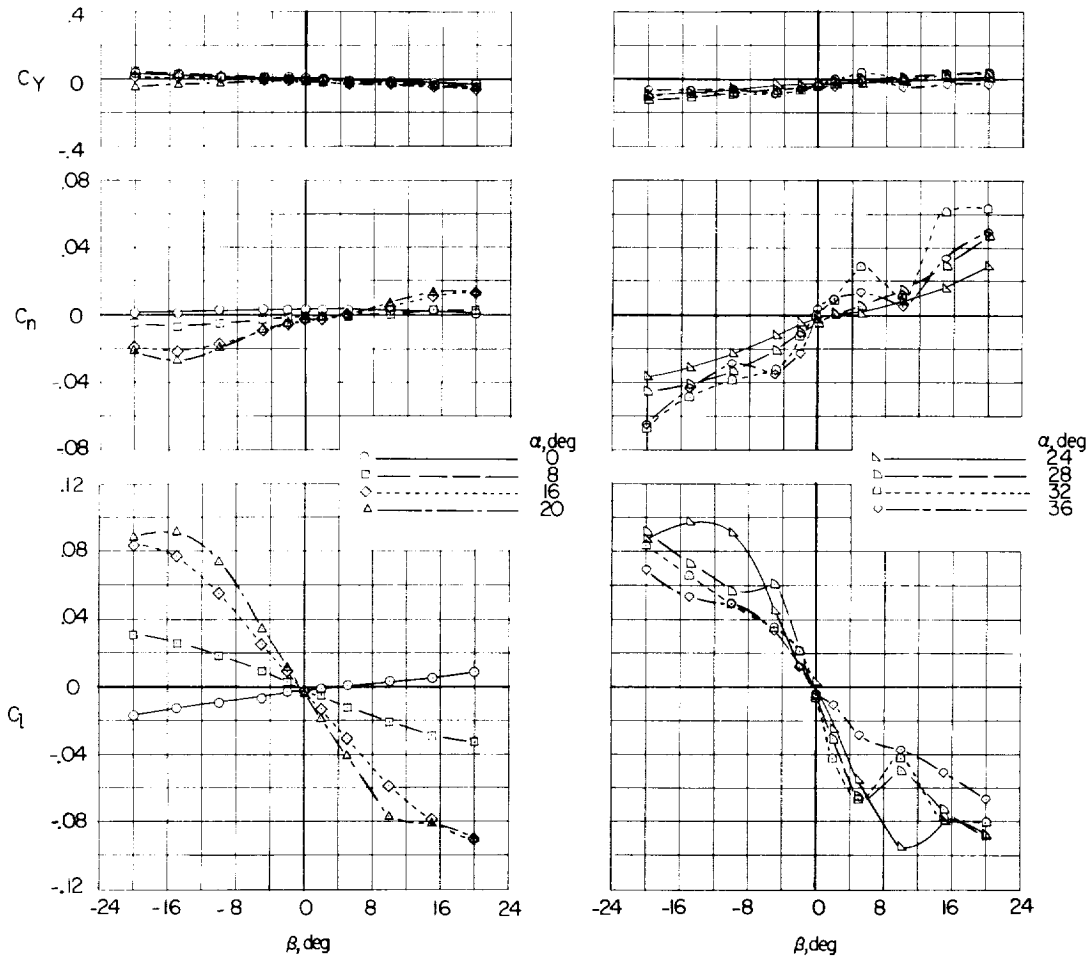

(c) Vertical tails off.

Figure 7.- Continued.

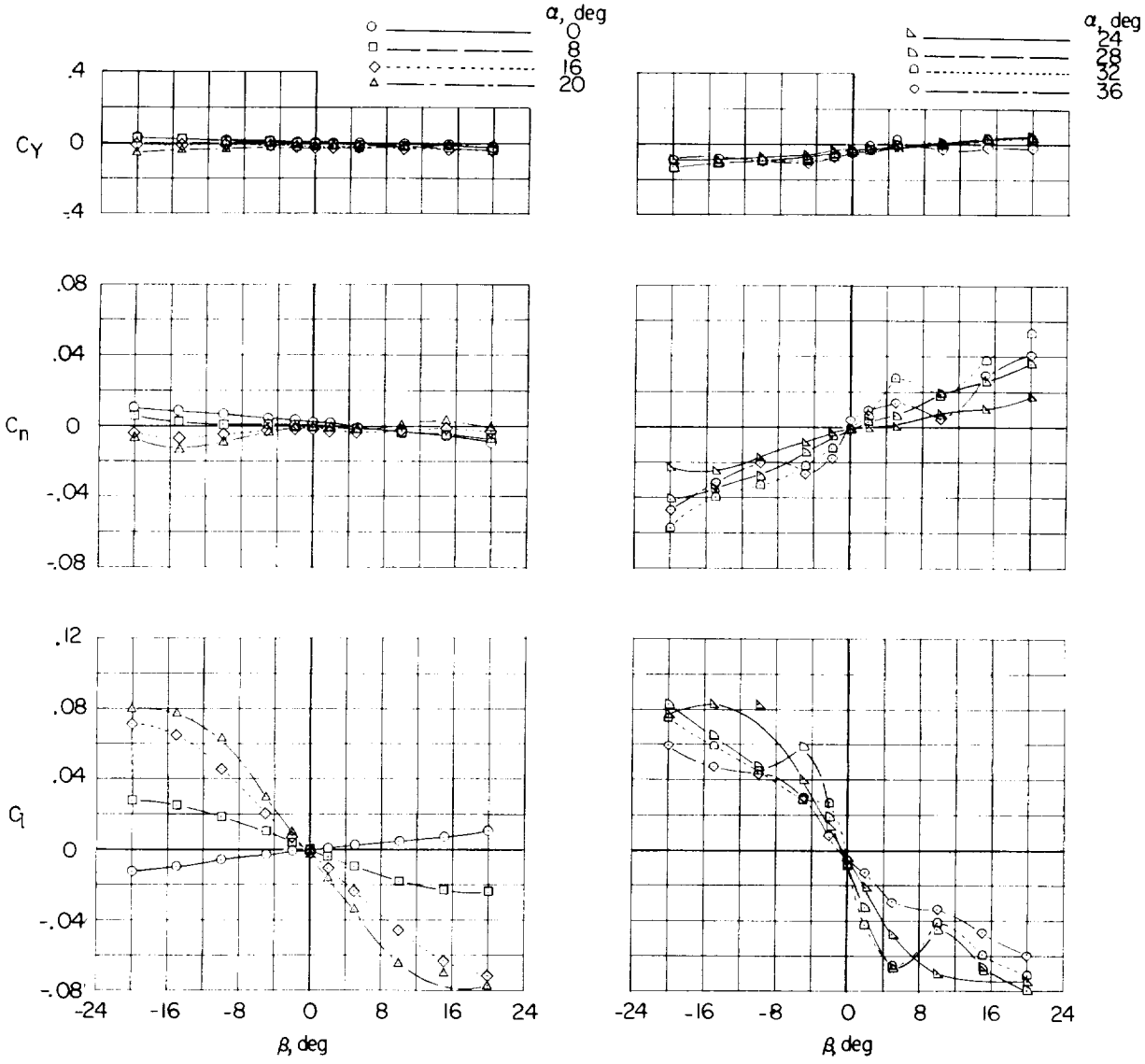

(d) Cones and vertical tails off.

Figure 7.- Concluded.

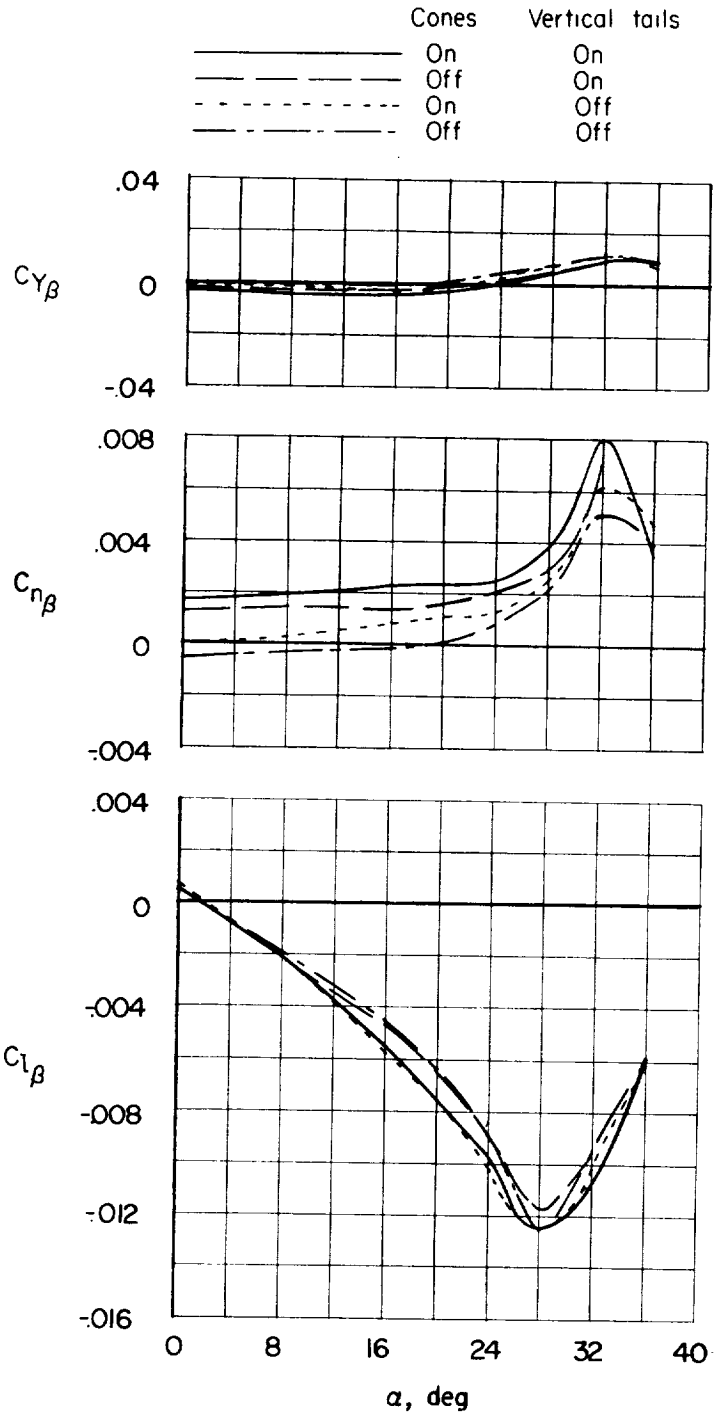

Figure 8.- Variation of static lateral stability derivatives with angle of attack. $\beta = \pm 5^{\circ}$; plotted per degree.

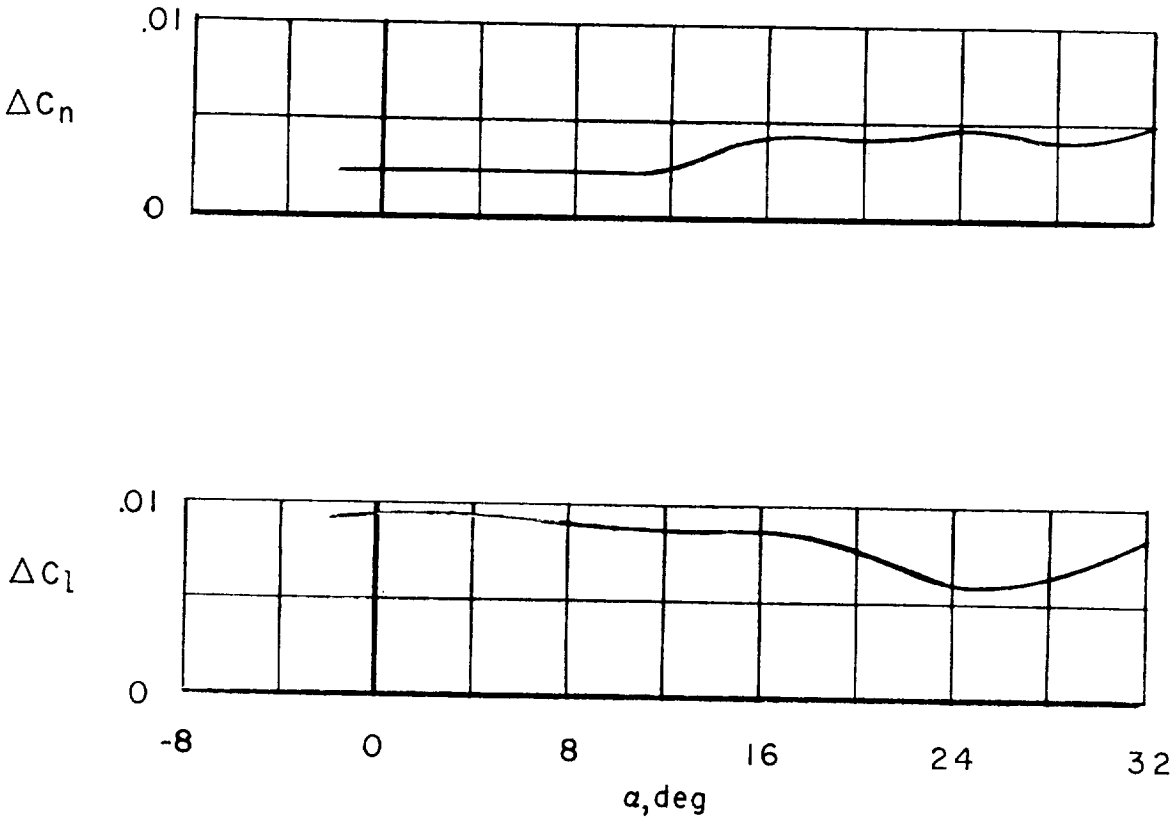

Figure 9.- Incremental yawing- and rolling-moment coefficients due to aileron deflection of ±5°. Cones on; $\beta = 0°$; $\delta_e = 0°$.

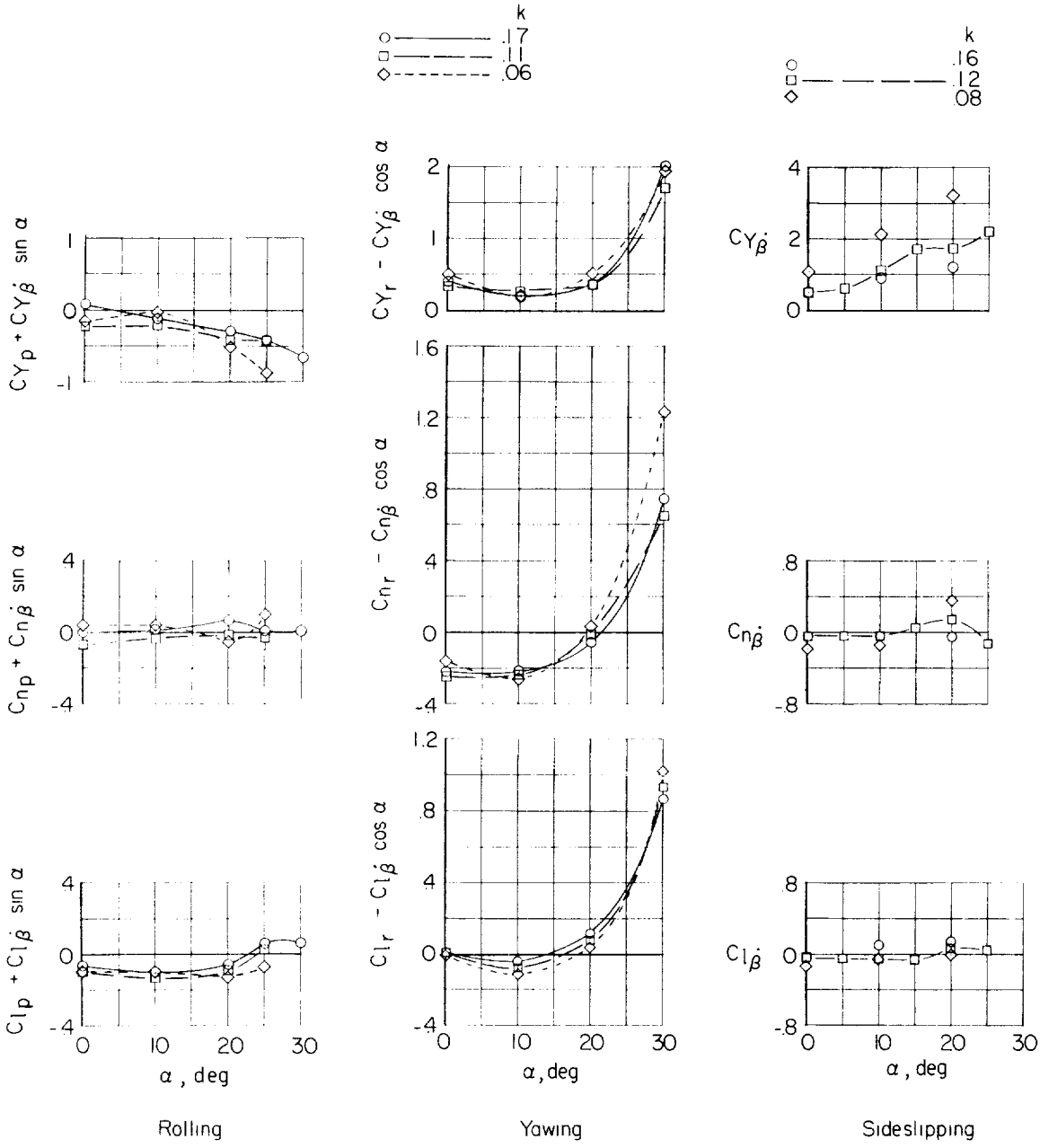

Figure 10.- Variation of out-of-phase derivatives with angle of attack. Cones off; $\delta_e = 0^\circ$; plotted per radian.

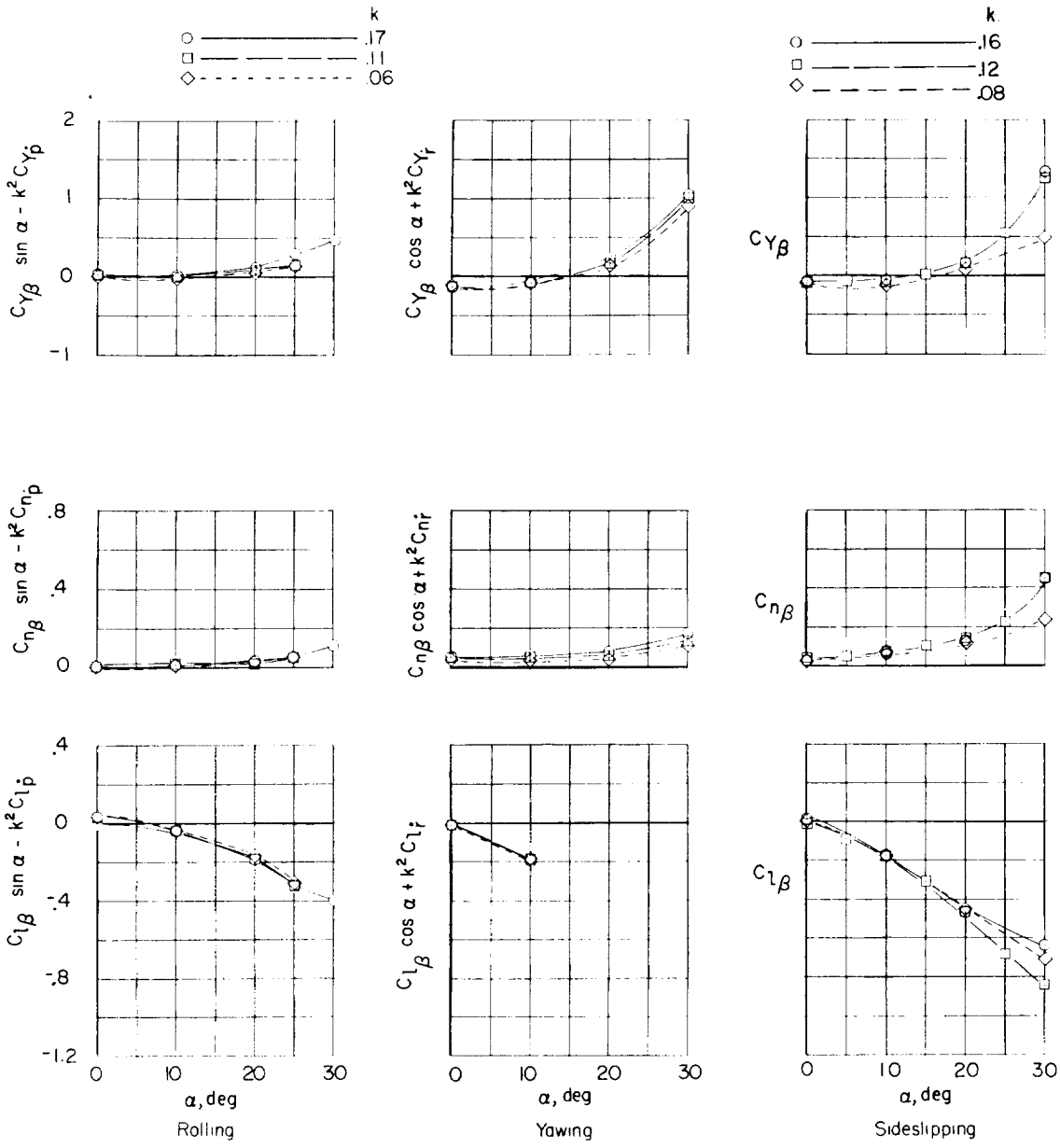

(a) Rolling. (b) Yawing. (c) Sideslipping.

Figure 11.- Variation of in-phase derivatives with angle of attack. Cones off; $\delta_e = 0^\circ$; plotted per radian.

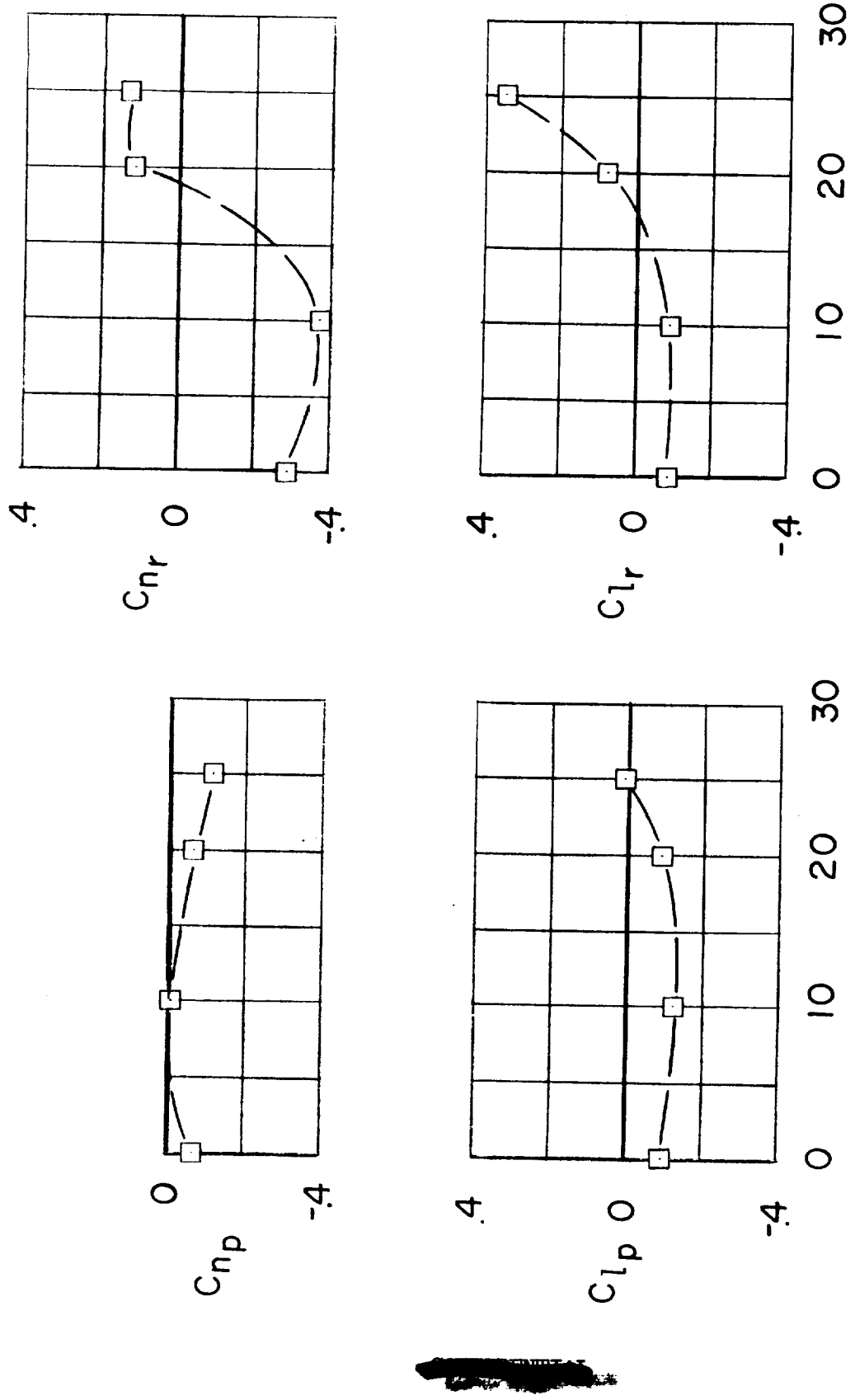

Figure 12.- Variation of rolling- and yawing-velocity derivatives with angle of attack as determined from k = 0.12 data of figure 10. Cones off.

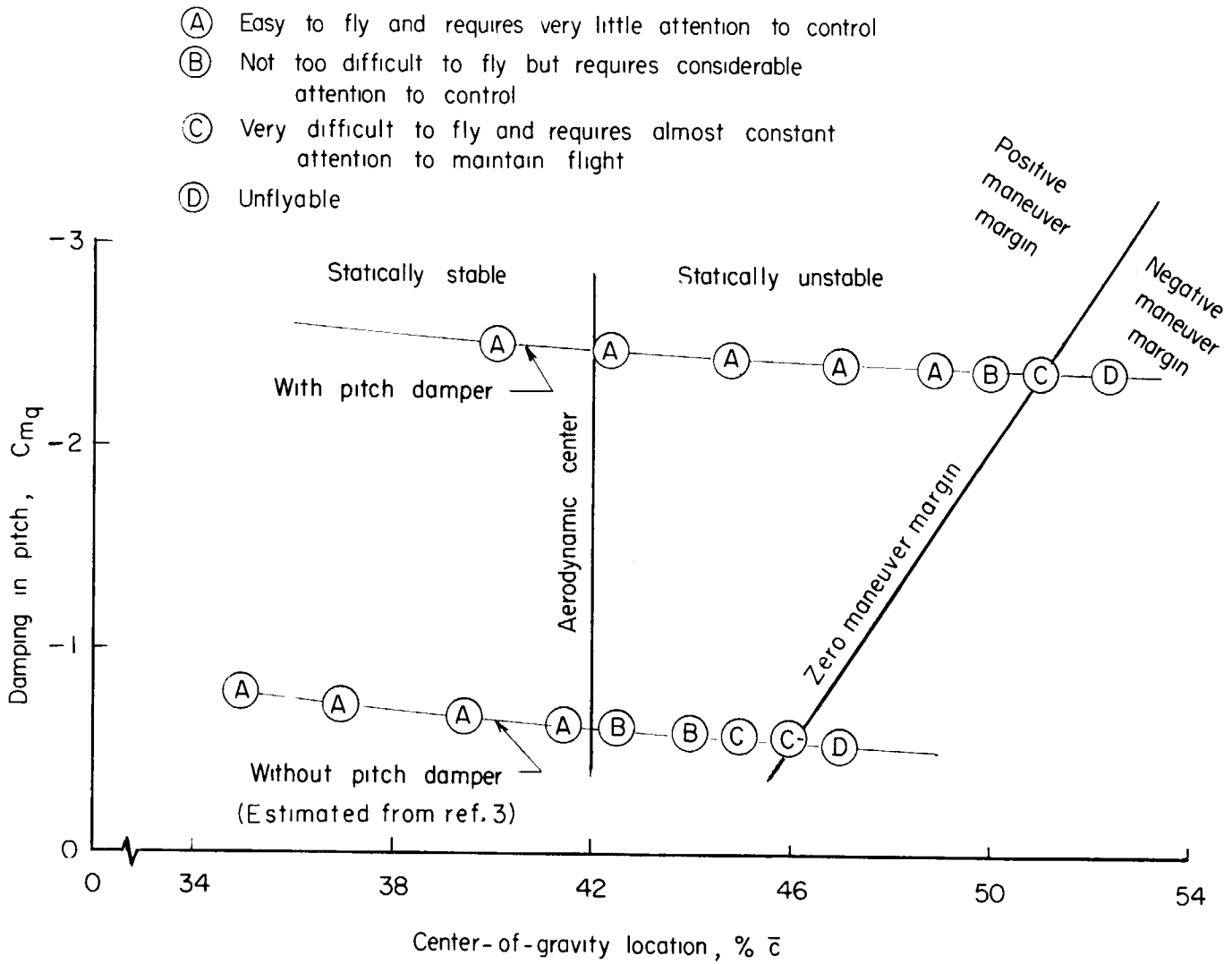

Figure 13.- Effect of damping in pitch and center-of-gravity location on the longitudinal flight characteristics of model. Cones off; $\alpha = 16^{\circ}$; $\delta_e = \pm 5^{\circ}$.